Dependence of the Yb^{3+} emission cross section and lifetime on temperature and concentration in yttrium aluminum garnet

Jun Dong and Michael Bass

School of Optics and Center for Research and Education in Optics and Lasers, University of Central Florida, Orlando, Florida 32816-2700

Yanli Mao, Peizhen Deng, and Fuxi Gan

Shanghai Institute of Optics and Fine Mechanics, Chinese Academy of Sciences, Shanghai 201800, China

Received November 5, 2002; revised manuscript received April 28, 2003

Measurements are reported of the spectroscopic properties (absorption and emission spectra, stimulated-emission cross section, and radiative lifetime) of $(Yb_xY_{1-x})_3Al_5O_{12}$ for nominal x values of 0.025, 0.05, 0.1, 0.2 and 0.3 at temperatures of 15–300 K. The emission cross sections of Yb:YAG with different Yb^{3+} concentrations were determined by use of the Füchtbauer–Ladenburg formula and the reciprocity method. At low temperatures, the product ($\sigma\tau$) of the effective stimulated-emission cross section and the radiative lifetime is greater than at room temperature for all concentrations. Product $\sigma\tau$ is nearly independent of Yb^{3+} concentration at a given temperature. These results will aid in the design of high-power thin disk lasers by use of highly doped Yb:YAG. © 2003 Optical Society of America

OCIS codes: 140.3580, 300.6280.

1. INTRODUCTION

The rapid development of InGaAs laser diodes emitting from 0.9 to 1.0 μm (Refs. 1 and 2) has made high-average-power lasers based on Yb:YAG crystals feasible. InGaAs diodes permit direct pumping of the 941-nm absorption band of Yb:YAG. End-, face- and side-pumped Yb:YAG lasers have been demonstrated with high efficiencies and high average output power.[3–9] The advantages of the Yb^{3+} ion as a lasant ion derive from its simple electronic structure. There are only two energy-level manifolds, the ground $^2F_{7/2}$ state and an excited $^2F_{5/2}$ state, which are separated by approximately 10,000 cm^{-1}. Effects such as excited-state absorption, cross relaxation, upconversion, and concentration quenching are absent from this lasant. These processes are present in other rare-earth ions used as lasant ions and can lead to reduced laser efficiencies because alternative paths exist to deplete the excited-state population. The Yb^{3+} ion, lasing at $\sim$1.03 μm, also has a small quantum defect that results in a small amount of pump power's being deposited as heat in the gain medium. Further, the host $Y_3Al_5O_{12}$ (YAG) is optically isotropic, has high thermal conductivity, and is mechanically robust. Together these features make Yb:YAG an attractive candidate for high-average-power applications.

An additional attractive advantage of Yb^{3+} dopant ions is that they can be incorporated into YAG at high concentrations. Certain laser architectures, such as thin disk and waveguide designs, can benefit from highly doped solid-state laser materials because highly doped materials can absorb pump light in thin gain media. For instance, in thin disk lasers the fracture limit scales as the inverse of the thickness of the gain medium. Therefore keeping the gain medium thin while maintaining sufficient rare-earth ion density to absorb the pump light facilitates higher absorbed pump power density, higher efficiencies, and improved thermal management. Another advantage that Yb:YAG offers is that its wide absorption band centered at 941 nm ($\sim$18-nm FWHM) is more accepting of pump diode laser wavelength variations[9] than is Nd-doped YAG pumped at 808 nm.

The main disadvantage of Yb-doped hosts is their quasi-three-level nature caused by the thermal population of the higher levels of the $^4F_{7/2}$ lower lasing level at $\sim$612 cm^{-1} above the ground level. This thermal population has deleterious effects on the resonant reabsorption of laser emission by the thermally populated lower-laser-level Stark state, which contains $\sim$5% of the $^4F_{7/2}$ population at room temperature. Therefore it is difficult to obtain population inversion at room temperature; the lasing threshold is high and the lasing efficiency is consequently low. One achieves efficient population inversion by either pumping at high pump power intensities at 300 K (1.5–10 kW/cm^2) (Ref. 10) or by depopulation of the highest Stark components of the ground state. The latter option is achieved by cooling of the system to temperatures at which only the lowest Stark levels are thermally populated.

The effective stimulated-emission cross section (σ) and radiative lifetime (τ) are two important parameters for the assessment of a laser crystal. Knowledge of both σ and τ is essential in evaluating laser system performance parameters such as saturation intensity and threshold pump power. For example, the threshold pump power is

0740-3224/2003/091975-05$15.00

inversely proportional to the product of the effective emission cross section and the radiative lifetime of the lasing crystal.[11] Knowledge of the stimulated-emission cross section and the radiative lifetime of Yb in YAG crystals with different concentrations at different temperatures is essential to the selection of the proper material for use in laser systems. Unfortunately, there have been to our knowledge no systematic measurements of these parameters. Patel *et al.*[12] reported lifetime measurements of Yb:YAG crystals with various concentrations at room temperature and considered reabsorption and radiative trapping. However, they did not measure the emission cross section. Sumida and Fan[13] reported emission cross-section and lifetime measurements of 5.5 at. % Yb:YAG as a function of temperature in the range 80–400 K, but they did not consider the variation of emission cross section and lifetime with different Yb^{3+} concentrations. In this paper we report experimental measurements of the emission cross section, 1.03-μm linewidth, peak wavelength, and the 1.03-μm radiative lifetime for several Yb^{3+} concentrations of Yb:YAG over a temperature range appropriate for many potential laser applications. The effect of Yb^{3+} concentration and temperature on these parameters is evaluated. The product of the emission cross section and the radiative lifetime, $\sigma\tau$, is found experimentally to be nearly independent of concentration, though it varies with temperature. These data allow the laser designer more flexibility in choosing the concentration of Yb:YAG for use in a laser. For example, in a high-power thin disk laser a high-concentration gain medium might be desirable because it will absorb pump light incident through the disk's face more effectively than will a lower-concentration material.

2. EXPERIMENTS

Yb:YAG crystals doped with 2.5, 5, 10, 20, and 30 at. % Yb^{3+} were grown by the Czochralski method. Inasmuch as the radius of Yb^{3+} ions (0.0985 nm) is nearly the same as that of Y^{3+} ions (0.1019 nm), the Yb^{3+} distribution coefficient for YAG crystal growth is nearly unity, so the concentrations of Yb^{3+} in the YAG crystals listed are the concentrations of Yb^{3+} in the melt. This assumption is supported by the relative strengths of the measured absorption spectra of the various Yb:YAG crystals. Samples for spectroscopic and lifetime measurements of 10mm $\times$ 10mm $\times$ 2 mm were cut out of the boules with the largest the surfaces oriented normal to the $\langle 111 \rangle$ growth axis. These surfaces were polished, whereas the 10mm $\times$ 2 mm surfaces were fine ground.

Room-temperature absorption spectra were measured with a Cary 500 Scan UV-Vis-NIR spectrophotometer. Emission spectra were measured at 950–1100 nm with a fiber-coupled diode laser operating at 943 nm as the pump source. The pump light was focused into one of the ground surfaces of the sample close to the polished surface through which the emitted fluorescence was to be observed. As a result the fluorescent light detected was generated close to the surface from which it exited the sample, such that it experienced minimal radiation trapping. The excitation signal was monitored during the experiment with a silicon detector. An indium gallium arsenide (InGaAs) detector located at the output slit of a 25-cm focal-length Jarrell–Ash monochromator was used to detect the fluorescence emission spectral intensity. With 50-μm slits the resolution of this detection system was ~0.4 nm. Before their use in calculating the stimulated-emission cross section, the recorded spectra were corrected for the spectral response of the detector and of the monochromator grating. Calibration of the detection system was achieved by recording of its response to light from a tungsten–iodine white-light source that had been calibrated at the National Institute for Standards and Testing.

The excitation source for emission lifetime measurements was a single-frequency (linewidth, 0.2 cm^{-1}), tunable optical parametric oscillator (Quanta Ray MOPO-SL) tuned to 943 nm. Its pulse duration was ~5 ns. The energy of the idler pulse delivered by the optical parametric oscillator at 941 nm is $\leq$2 mJ. Fluorescence from the Yb:YAG samples was collected with an $f = 5$ cm lens and dispersed with the 25-cm focal-length Jarrell–Ash monochromator. An InGaAs photodiode connected to a preamplifier was used to detect the intensity of the fluorescence emission. Decay curves were recorded with a Tektronix 2440 500-Ms/s digital oscilloscope and a computer-controlled data acquisition system. The emission spectra and lifetime measurements were carried out at temperatures of 15–300 K in a temperature-controlled compressed helium cryostat.

3. RESULTS AND DISCUSSION

Absorption spectra of Yb:YAG for five Yb^{3+} concentrations at room temperature are shown in Fig. 1. The maximum absorption in the 850–1070-nm wavelength range is at 941 nm, at which commercial Al-free InGaAs laser diodes are available as pump sources. With increasing Yb^{3+} concentration, the absorption coefficient at 941 nm increases from 2.78 cm^{-1} for a 2.5-at. % Yb^{3+} concentration to 31 cm^{-1} for 30 at. %. There is self-absorption at the lasing wavelength of 1.03 μm in the Yb:YAG crystals at room temperature.

Representative emission spectra of 10-at. % Yb:YAG at room temperature and at 70 K are shown in Fig. 2. At 77

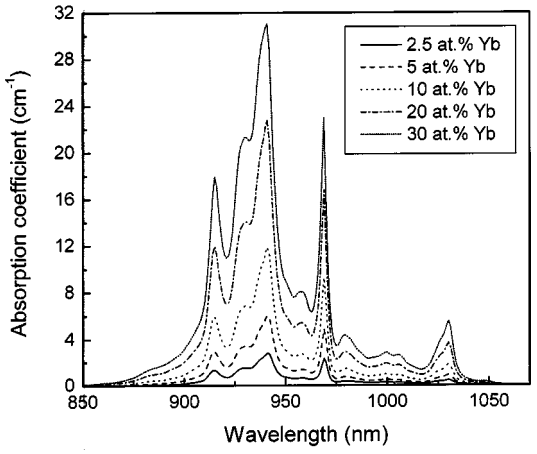

Fig. 1. Absorption spectra of Yb:YAG with five Yb concentrations at room temperature.

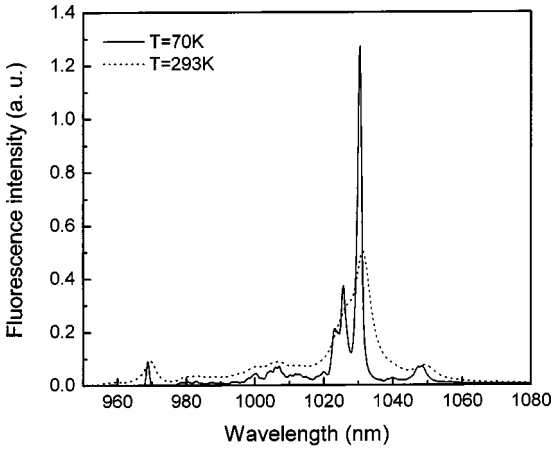

Fig. 2. Emission spectra of 10-at. % Yb:YAG at 70 K and at room temperature (293 K).

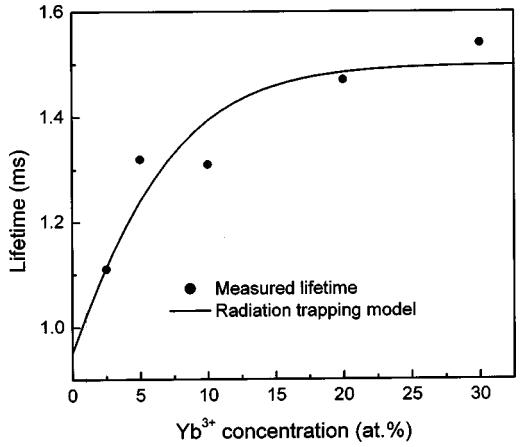

Fig. 3. Measured room-temperature fluorescent lifetime of Yb^{3+} ions in YAG as a function of concentration. The solid curve is the functional form for this dependence that is due to radiation trapping as given in Ref. 15 with 969-nm branching ratio β=0.366 and geometric scaling factor γ=0.203 used as fitting parameters.

K the emission strength is greater and the line shape of the emission line shape becomes narrower.

The main disadvantage of Yb:YAG as a laser is that it is a quasi-three-level system and consequently experiences reabsorption loss as a result of the significant population in the lower laser level at room temperature. For such systems radiation trapping by single centers or pairs takes place and can lead to a considerable increase in the measured fluorescence lifetime.[14] In fact, as shown in Fig. 3, we fitted our measured fluorescence lifetime data at room temperature as a function of concentration to the model given in Ref. 15. Although the fitting process required adjustment of two parameters and is thus not completely satisfying, it did indicate the presence of radiation trapping. We note that there is good agreement between our measured fluorescence lifetimes and the model from Ref. 15 that uses as fitting parameters the 969-nm branching ratio β (=0.366) and the geometric scaling factor γ (=0.203). As indicated in the description of the experiments, the geometry of the sample and the detection scheme were chosen to minimize radiation trapping.

We must keep radiation trapping in mind when we try to determine the radiative lifetime of the Yb^{3+} ions because, according to the Fuchtbauer–Ladenburg (F–L) formula, the effective emission cross section is inversely proportional to the radiative lifetime. The fluorescence-lifetime data for all samples at all temperatures were characterized by a single exponential decay function. Figure 4 shows the relationship of the measured fluorescence lifetime of Yb:YAG crystals to temperature. At higher temperatures (above 200 K), the fluorescence lifetime increases as the Yb^{3+} concentration increases in the YAG host because of radiative trapping and reabsorption effects. The measured lifetime is longer than the radiative lifetime in these cases. At lower temperatures (below 80 K), the measured fluorescence lifetime of Yb in YAG is nearly the same for each concentration, similar to the results reported by Patel *et al.*,[12] except for the 30-at. % Yb:YAG crystal. The measured 77-K lifetime of the several Yb:YAG crystals is the radiative lifetime that we use in evaluating the stimulated-emission cross section by using the F–L formula. The decreased lifetime observed for the 30-at. % crystal at the lowest temperatures may be due to the presence of more impurities in the highly doped crystal, which cause significant fluorescence quenching. These impurities can be other rare-earth ions that are hard to eliminate from the Yb starting material.

The ytterbium emission from YAG is not polarization dependent, so one could use the emission spectra obtained to calculate the effective stimulated emission cross section of an Yb^{3+} ion from the manifold ${}^2F_{5/2} \rightarrow {}^2F_{7/2}$ transitions in Yb:YAG by applying the F–L formula. The fundamental relationship between spontaneous-emission distribution $E_{(\lambda)} = I(\lambda)/\int I(\lambda)d\lambda$ (integrating over all ${}^2F_{5/2} \rightarrow {}^2F_{7/2}$ transitions) and stimulated emission cross section distribution $\sigma_{\mathrm{em}}(\lambda)$ is

$$\sigma_{\mathrm{em}}(\lambda) = \frac{1}{8\pi}\frac{\lambda^5}{n^2 c\tau}\frac{I(\lambda)}{\int I(\lambda)\lambda d\lambda}, \tag{1}$$

where τ is the radiative lifetime of the upper laser level, c is the velocity of light in vacuum, and n is the refractive

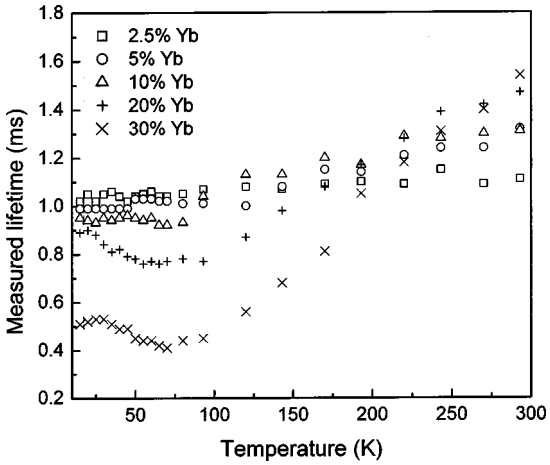

Fig. 4. Measured lifetimes of Yb:YAG crystals as a function of temperature.

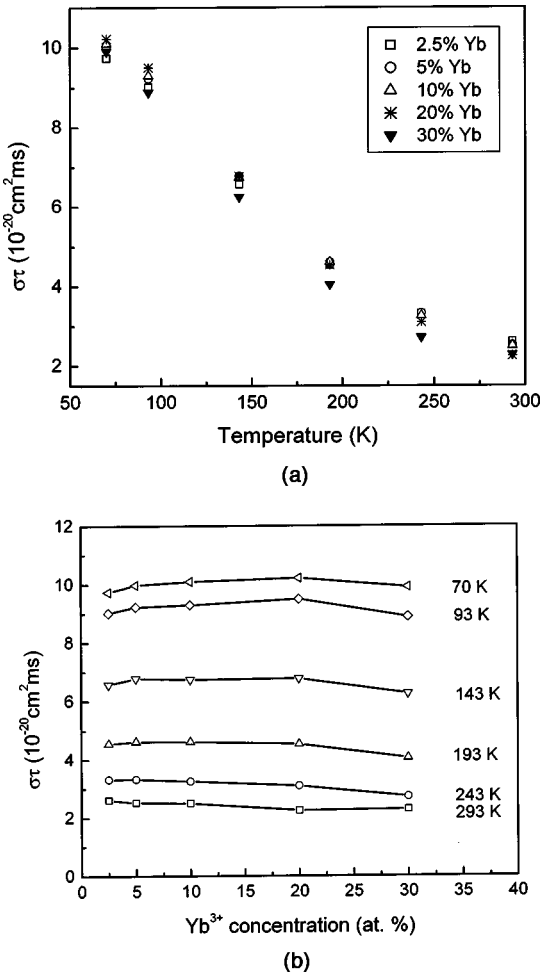

Fig. 5. (a) Measured product $\sigma\tau$ of Yb:YAG crystals for (a) five Yb^{3+} ion concentrations as a function of temperature and (b) six temperatures as a function of the concentration of Yb^{3+} ions.

index at the emission wavelength (at 1030 nm, n is $\sim$1.82), and $I(\lambda)$ is the corrected emission spectral intensity of emission of the Yb^{3+} ions.

From Eq. (1) we can calculate the product $\sigma\tau$ at the peak lasing wavelength as determined by the measured emission spectra of the differently doped Yb:YAG crystals at different temperatures without knowing the actual radiative lifetime. That product $\sigma\tau$ is given by

$$\sigma\tau = \frac{1}{8\pi}\frac{\lambda^5}{n^2 c}\frac{I(\lambda)}{\int I(\lambda)\lambda d\lambda}$$

at the peak lasing wavelength of 1.03 μm. The measured products $\sigma\tau$ at peak lasing wavelength of the several concentrations of Yb:YAG crystals are shown as functions of temperature in Fig. 5(a). Figure 5(b) shows clearly that product $\sigma\tau$ is nearly independent of Yb concentration at each temperature. Our data also show that $\sigma\tau$ increases as the temperature decreases from 2.4×10^{-20} cm^2 ms at room temperature to 10×10^{-20} cm^2 ms at 70 K.

These data benefit the design of thin disk lasers chosen to minimize thermal-gradient-induced stresses. Lasing properties are determined by product $\sigma\tau$, and the ability to select concentration without sacrificing lasing performance may enable pump thin disk Yb:YAG lasers to absorb pump power efficiently. Higher-concentration material has higher absorption, so pump light can be deposited in the two passes through a coated thin disk without the need to use complex multiple reflecting mirrors. The most interesting thing about these lasers is that $\sigma\tau$ is large at liquid-nitrogen temperature, which is approximately five times room temperature. Thus, if the thin disk laser is operated at liquid-nitrogen temperature, the threshold pump power will be significantly reduced and the saturation intensity lowered, so power can be extracted efficiently.

Using the measured lifetime at the lowest temperature as the radiative lifetime of different concentrations of Yb:YAG crystals, we calculated the effective emission cross section of Yb:YAG crystals from the F–L formula [Eq. (1)]. Figure 6 shows the dependence of the effective emission cross section of these Yb:YAG crystals on temperature. The emission cross section increases as the temperature decreases. We also calculated the emission cross section by using the reciprocity method according to the measured absorption spectra at room temperature. The calculated emission cross section for various Yb:YAG crystals at room temperature measured by the reciprocity method is approximately 2.3×10^{-20} cm^2 and is in a good agreement with the emission cross section obtained with the F–L formula. We note that the difference between our room-temperature cross section and that given in Ref. 14 may be due to our use of the measured 77-K lifetime for the radiative lifetime of the transition. This lifetime is smaller than that measured at room temperature, and the resultant cross section that we found is larger.

The dependence on temperature of the peak linewidth (FWHM) near 1030 nm and of the peak emission wavelength are shown in Figs. 7 and 8, respectively. For all samples, as the temperature increases from 70 K to room temperature the peak linewidth (FWHM) and the peak wavelength increase. The peak wavelength shifts by $\sim$ 0.6 nm. The peak linewidth (FWHM) near 1030 nm depends strongly on temperature, decreasing to $\sim$1.5 nm at liquid-nitrogen temperature compared with its room-temperature value of $\sim$10 nm.

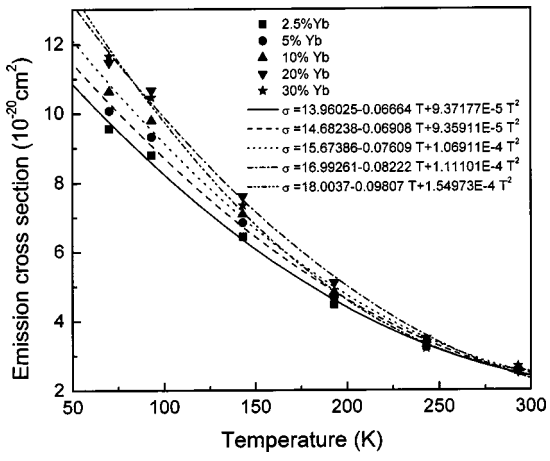

Fig. 6. Emission cross sections of Yb:YAG as a function of temperature for five concentrations of Yb. The indicated polynomial fits were obtained by the least-squares method.

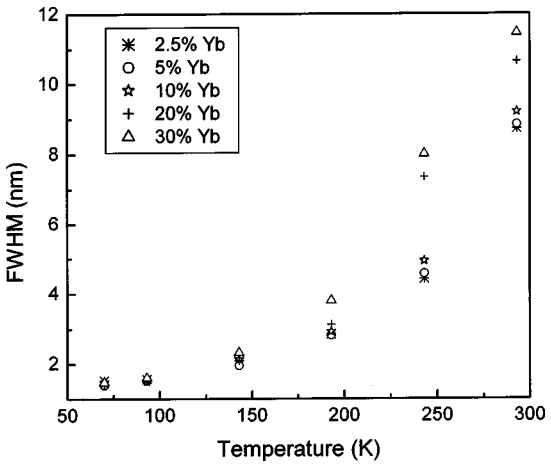

Fig. 7. Linewidths (FWHM) near the peak lasing wavelength of Yb:YAG as a function of temperature for five concentrations of Yb.

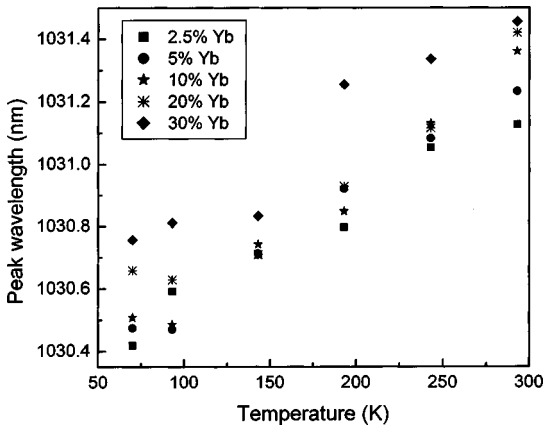

Fig. 8. Peak lasing wavelengths of Yb:YAG as a function of temperature for five concentrations of Yb.

4. CONCLUSIONS

We obtained products $\sigma\tau$ of Yb:YAG crystals doped with various Yb concentrations by using the Fuchtbauer–Ladenburg formula over a temperature range from liquid-nitrogen temperature to room temperature. We found that products $\sigma\tau$ of Yb:YAG crystals are nearly independent of Yb concentration. This result suggests the use of highly doped Yb:YAG thin disks to absorb pump power effectively without sacrificing lasing performance. The products $\sigma\tau$ of Yb:YAG crystals increase with decreasing temperature, benefitting Yb:YAG laser operation at liquid-nitrogen temperature. The fluorescence-lifetime measurements show that the effect of reabsorption and radiative trapping is significant for a quasi-three-level Yb:YAG system and leads to an underestimation of the emission cross section, especially for highly doped Yb:YAG crystals (>20 at. %).

ACKNOWLEDGMENTS

This research was supported by the National Natural Science Foundation of China under project 6998806 and by the National 863-416 Foundation of China. Support for the research in the United States was obtained through a grant from Raytheon Company.

M. Bass's e-mail address is bass@creol.ucf.edu.

REFERENCES

1. D. P. Bour, D. B. Gilbert, K. B. Fabian, J. P. Bednarz, and M. Ettenberg, "Low degradation rate in strained InGaAs/AlGaAs single quantum well lasers," IEEE Photon. Technol. Lett. **2**, 173–174 (1990).
2. S. L. Yellin, A. H. Shepard, R. J. Dalby, J. A. Baumaum, H. B. Serreze, T. S. Guide, R. Solarz, K. J. Bystrom, C. M. Harding, and R. G. Walters, "Reliability of GaAs-based semiconductor diode lasers: 0.6–1.1 μm," IEEE J. Quantum Electron. **29**, 2058–2067 (1993).
3. R. J. Beach, "cw theory of quasi-three level end-pumped laser oscillators," Opt. Commun. **123**, 385–393 (1996).
4. C. Bibeau, R. J. Beach, S. C. Mitchell, M. A. Emanuel, J. Skidmore, C. A. Ebbers, S. B. Sutton, and K. S. Jancaitis, "High-average-power 1-μm performance and frequency conversion of a diode-end-pumped Yb:YAG laser," IEEE J. Quantum Electron. **34**, 2010–2019 (1998).
5. T. Y. Fan, S. Klunk, and G. Henein, "Diode-pumped *Q*-switched Yb:YAG laser," Opt. Lett. **18**, 423–425 (1993).
6. P. Lacovara, H. K. Choi, C. A. Wang, R. L. Aggarwal, and T. Y. Fan, "Room-temperature diode-pumped Yb:YAG laser," Opt. Lett. **16**, 1089–1091 (1991).
7. E. C. Honea, R. J. Beach, S. C. Mitchell, J. A. Skidmore, M. A. Emanuel, S. B. Stutton, S. A. Payne, P. V. Avizonis, R. S. Monroe, and D. G. Harris, "High-power dual-rod Yb:YAG laser," Opt. Lett. **25**, 805–807 (2000).
8. T. S. Rutherford, W. M. Tulloch, E. K. Gustafson, and R. L. Byer, "Edge-pumped quasi-three-level slab lasers: design and power scaling," IEEE J. Quantum Electron. **36**, 205–219 (2000).
9. H. W. Brusselbach, D. S. Sumida, R. A. Reeder, and R. W. Byren, "Low-heat high-power scaling using InGaAs-diode-pumped Yb:YAG lasers," IEEE J. Sel. Top. Quantum Electron. **3**, 105–116 (1997).
10. X. Giesen, H. Hugel, A. Voss, K. Witting, U. Brauch, and H. Opower, "Scalable concept for diode-pumped high-power solid-state lasers," Appl. Phys. B **58**, 365–372 (1994).
11. T. Y. Fan and R. L. Byer, "Diode laser pumped solid-state laser," IEEE J. Quantum Electron. **24**, 895–912 (1988).
12. F. D. Patel, E. C. Honea, J. Speth, S. A. Payne, R. Hutcheson, and R. Equall, "Laser demonstration of $Yb_3Al_5O_{12}$ (YbAG) and materials properties of highly doped Yb:YAG," IEEE J. Quantum Electron. **37**, 135–144 (2001).
13. D. S. Sumida and T. Y. Fan, "Emission spectra and fluorescence lifetime measurement of Yb:YAG as a function of temperature," in *Advanced Solid-State Lasers*, T. Y. Fan and B. H. T. Chai, eds., Vol. 20 of OSA Proceedings Series (Optical Society of America, Washington, D.C., 1994), pp. 100–102.
14. D. S. Sumida and T. Y. Fan, "Effect of radiation trapping on fluorescence lifetime and emission cross section measurements in solid-state media," Opt. Lett. **19**, 1343–1345 (1994).
15. C. D. Marshall, S. A. Payne, L. K. Smith, H. T. Powell, W. F. Krupke, and B. H. T. Chai, "1.047-μm Yb:$Sr_5(PO_4)_3F$ energy storage optical amplifier," IEEE J. Sel. Top. Quantum Electron. **1**, 67–77 (1995).